Armenian Journal of Mathematics
Volume 14, Number 13, 2022, 1–12
https://doi.org/10.52737/18291163-2022.14.13-1-12

Bifurcation Analysis of a Piecewise Smooth Map with Two Asymptotes

R. Makrooni

Abstract. In this paper, we consider a discontinuous piecewise smooth system involving four parameters and two asymptotes, recently introduced as a model in engineering sciences. We classify and investigate its bifurcation behaviour. A local bifurcation analysis of the system in the range of parameters which has not been studied so far is undertaken and then supported by numerical computations. This reveals the existence of a flip bifurcation depends on the power singularity. Moreover, we state that a set of positive measure of points with divergent dynamic behaviour exists.

Key Words: Discontinuous System, Divergence, Flip Bifurcation, Periodic Orbit
Mathematics Subject Classification 2010: 37C83, 37G15, 37N99

Introduction

Traditional analysis of dynamical systems has restricted its attention to smooth problems. It has become increasingly clear that there are distinctive phenomena unique to discontinuous systems that can be analyzed mathematically but which fall outside the usual methodology for smooth dynamical systems. Hence, it is of primary importance to study piecewise smooth dynamical systems, continuous or discontinuous, and investigate their bifurcation structures (see, for instance, [6, 8]). In piecewise smooth (PWS for short) systems, the discrete phase space is divided into compartments within which the map is smooth, and the compartments are separated by border lines at which the map may not be differentiable [6]. These systems represent a large number of engineering systems with nonsmooth vector fields. Their applications include switching electronic circuits [3], impacting mechanical systems [18, 22], stick-slip oscillations [5], piecewise smooth nonlinear oscillators [19, 20], cardiac dynamics [4, 12], etc.

The studies on the dynamics of PWS maps have mostly been done using a piecewise linear approximation in the neighbourhood of the border [1, 2, 11]. However, many applications in engineering and control strategies demand one to predict the behaviour by including the nonlinearities in the map, at least up to the leading-order term. For example, in the most famous Nordmark systems associated with grazing bifurcations, the leading order term in the nonlinear side has the power of 1/2 (see [18]). In this case, the normal form mapping in the neighbourhood of the border is linear on one side and has a square-root term on the other. In analyzing the stick-slip motion with dry friction, it has been shown that the leading-order nonlinear term has a power of 3/2 (see [5]). For the normal form mapping of sliding bifurcations, the authors in [7] manifested the powers of 3/2, 2 and 3 in the leading-order nonlinear terms for different cases of sliding bifurcations. However, the dynamics of such PWS maps, where the function is linear in one of the partitions and nonlinear in the other, are still far from being understood.

Based on the above premise, we consider the PWS map in a generalized sense, given by

$$x \longmapsto f(x) = \begin{cases} f_L(x) = \alpha x + \mu & \text{if} \quad x \leq 0, \\ f_R(x) = \beta x^{-\gamma} + \mu & \text{if} \quad x > 0, \end{cases} \tag{1}$$

where the power of the nonlinear side γ can take any arbitrary real value and α, β and μ are real parameters.

In all the cases mentioned above, we can see that the power term in (1), which is obtained through a Taylor series expansion of a nonlinear function, can take only particular positive values. Hence, the system is a continuous PWS map (in general, for $\gamma < 0$) which has been studied for several years. Note that the map f in (1) with real negative power, that is to $\gamma > 0$, is a discontinuous PWS map in which the function $f_R(x)$, defined on the right branch, has a vertical asymptote at the discontinuity point $x = 0$. The discontinuous system has dynamic properties and bifurcations very much different from those happening in the continuous map. The main results for the discontinuous system, in both invertible and noninvertible cases, for the parameters $\beta < 0$ and $\mu > 0$ have been obtained recently in [9, 14, 15, 16, 17, 21]. The discontinuous case with $\mu < 0$ has been studied in [10]. However, in the discontinuous system, the classification of the possible different results of smooth and nonsmooth bifurcations, under parameter variation in the corresponding space, is still to be investigated. Due to its numerous applications in engineering systems, in this paper, we subject the discontinuous map f in (1) to multi-parametric bifurcation study for the various ranges $\beta > 0$ and $\mu > 0$, which have not been considered so far, exploring the dynamics of this family of maps and describing its bifurcation structure in a theoretical way with proper illustrations.

The paper is organized as follows. In Section 1, we provide some preliminaries and recall notations and basic concepts. In Section 2, main results about bifurcation structures of the system are presented analytically and illustrated explicitely. In Section 3, the existence of divegent dynamical behaviour is proved. Section 4 provides the conclusion.

1 One-dimensional discontinuous piecewise smooth map

The one-dimensional (1D) discontinuous map that we are interested in comes from an applied context. Recent applications in engineering lead to nonlinear piecewise smooth dynamical systems among which much attention has been given to the system first proposed by Nordmark (see [18]) and defined by (1) for $\mu > 0$. As can be seen in (1), it is linear on the left side of the border $x = 0$ and nonlinear with singularity of the power γ on the right side. The values of two sides at $x = 0$, $\mu = 0$ are defined as

$$f(0) = \begin{cases} f_-(0) = \alpha \cdot 0 = 0, \\ f_+(0) = \beta/0^\gamma = sign(\beta) \cdot \infty, \end{cases}$$

Thus, the piecewise map is discontinuous, and the gap on two sides of the border tends to infinity, leading to a map with a vertical asymptote which is not new in the literature (see, for example, [13, 23]). To investigate the dynamics of map f in (1), it is preferable to reduce the number of system's parameters. Without loss of generality, the value of the parameter μ can be scaled to $\mu = 0$, $\mu = +1$ or $\mu = -1$. Thus, for any $\mu > 0$, by using the transformation $(x, \alpha, \beta, \mu) \longrightarrow (x/\mu, \alpha, \beta\mu^{-\gamma-1}, 1)$ for the map in (1), we obtain the following map

$$x \longmapsto f(x) = \begin{cases} f_L(x) = \alpha x + 1 & \text{if} \quad x \le 0, \\ f_R(x) = \beta x^{-\gamma} + 1 & \text{if} \quad x > 0, \end{cases} \tag{2}$$

while for any $\mu < 0$, by applying the similar transformation $(x, \alpha, \beta, \mu) \longrightarrow (-x/\mu, \alpha, \beta(-\mu)^{-\gamma-1}, -1)$, we have the similar map with -1 instead of $+1$. Throughout this work, we investigate the dynamics of map f given in (2) in the following parameters' range

$$Range\ I = \{(\alpha, \beta, \gamma) : \ \alpha \in \mathbb{R}, \ \beta > 0, \ \gamma > 0\}.$$

Note that map f with $\mu = -1$ has been studied in [10].

In this parameters' region, function $f_R(x)$ is decreasing with the range $(1, +\infty)$, while function $f_L(x)$ is increasing when $\alpha > 0$ with the range $(-\infty, 1)$ and decreasing when $\alpha < 0$ with the range $(1, +\infty)$. In the case

$\alpha > 0$, map f in (2) is invertible, while for $\alpha < 0$ it is noninvertible. Note that 1D invertible maps can not be chaotic and may have simple dynamics.

We recall that by using the symbolic notation based on the letters L and R corresponding to the two partitions $I_L = (-\infty, 0]$, $I_R = (0, +\infty)$, respectively, we may associate to each trajectory its itinerary by using the letter L when a point belongs to the partition I_L and R when a point belongs to the partition I_R. The fixed points of map f are denoted by $x = x_L^* \in I_L$ and $x = x_R^* \in I_R$.

2 Local bifurcation analysis

A graphical representation exhibits the richness of the dynamics of map f given by (2). In some graphical representations of the dynamic behaviors of system f in (2), it may be useful to consider the parameter space in the complete range for the parameter β, which means $\beta \in (-\infty, +\infty)$, to emphasize the occurrence of relevant bifurcations (particularly bifurcations with codimension larger than one). Hence, the nonlinear transformation $S(\beta) = arctan(\beta)$ has been considered which maps an unbounded interval $(-\infty, +\infty)$ into a bounded one, $(-\pi/2, \pi/2)$. Fig. 1 shows the two-dimensional bifurcation diagram in the parameter space $(\alpha, S(\beta))$ at the fixed values $\gamma = 0.5$ in Fig. 1a and $\gamma = 1.5$ in Fig. 1b. Examples of map f are shown in Fig. 1c.

The colored regions in Fig. 1 represent sets of values of the parameters in which map f has an attracting cycle, and different colors are related to different periods ($n \leq 60$). White regions represent parameter sets at which we have either higher periodicity or chaos. Note that these regions are visible for the noninvertible case $\alpha > 0$ and $\beta < 0$.

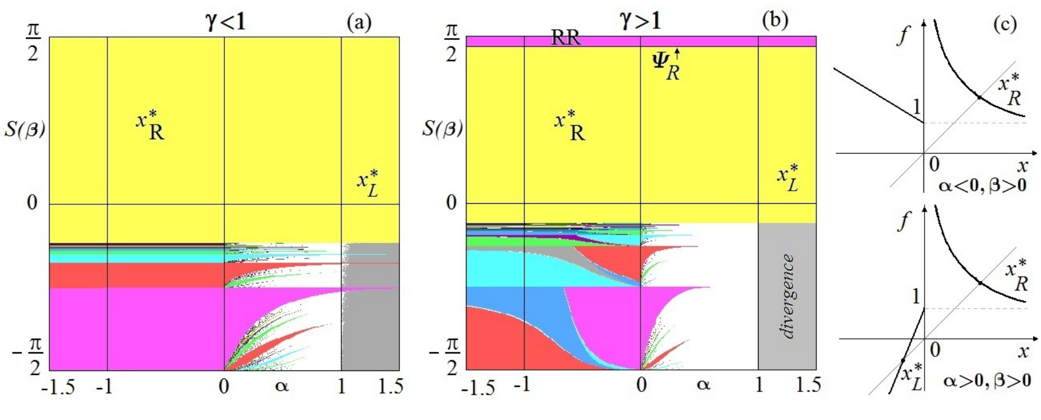

Figure 1: 2D bifurcation diagram of map f in $(\alpha, S(\beta))-$parameter plane. (a) $\gamma = 0.5$; (b) $\gamma = 1.5$; (c) examples of map f.

It can be seen instantly in Fig. 1 that the dynamics of map f is much simpler for $\beta > 0$ than for $\beta < 0$. Comparing Fig. 1a and Fig. 1b one can note that the bifurcation structure of map f depends also on the value of γ. In what follows, we explain the two different structures and what kind of transition occurs as the parameter γ varies through the value $\gamma = 1$.

The fixed point on the right side of the border exists for $\beta > 0$ and is expressed as follows.

Proposition 1 *Let $\alpha \in \mathbb{R}$, $\beta > 0$ and $\gamma > 0$. Then there exists a unique fixed point $x_R^* \in I_R$ for map f in (2), such that $1 < x_R^* < \beta + 1$.*

Proof. Regarding the equations of first and second derivatives of the function $f_R(x)$, we have that for $x > 0$, $f_R'(x) = -\beta\gamma x^{-\gamma-1} < 0$ and $f_R''(x) = \beta\gamma(\gamma+1)x^{-\gamma-2} > 0$. Thus, the function $f_R(x)$ is continuous, monotone decreasing and convex. Moreover, $\lim_{x\longrightarrow 0^+} f_R(x) = +\infty$, $\lim_{x\longrightarrow +\infty} f_R(x) = +1$ and $f_R(1) = \beta + 1 > 1$. Therefore, there exists $x_R^* \in I_R$ such that $f_R(x_R^*) = x_R^*$, that is,

$$\beta + (x_R^*)^\gamma = (x_R^*)^{\gamma+1}, \tag{3}$$

leading to $1 < x_R^* < \beta + 1$. □

The bifurcations of the fixed point x_R^* are described in the following

Theorem 1 *Let $\alpha \in \mathbb{R}$, $\beta > 0$ and $\gamma > 0$. For $0 < \gamma \leq 1$, the unique fixed point of map f in (2), namely $x_R^* \in I_R$, is globally attracting. For $\gamma > 1$, map f in (2) undergoes a smooth flip bifurcation at the fixed point x_R^* and at*

$$\beta = \frac{\gamma^\gamma}{(\gamma-1)^{\gamma+1}} := \beta_R^f. \tag{4}$$

In addition,

$$x_R^* \mid_{\beta=\beta_R^f} = \frac{\gamma}{\gamma-1} = x_{Rf}^*.$$

The fixed point x_R^* is repelling for $\beta > \beta_R^f$ and globally attracting for $0 < \beta \leq \beta_R^f$.

Proof. Considering the derivative function $f_R'(x) = -\beta\gamma/x^{\gamma+1} < 0$ and using equation (3) we obtain

$$f_R'(x_R^*) = -\frac{\beta}{(x_R^*)^\gamma}\frac{\gamma}{x_R^*} = -\left(1 - \frac{1}{x_R^*}\right)\gamma. \tag{5}$$

From $0 < 1 - 1/x_R^* < 1$, we have that for $0 < \gamma \leq 1$, the fixed point is attracting. On the other hand, for $\gamma > 1$, the fixed point x_R^* may be attracting or repelling. Due to the nonlinearity, the fixed point on the right side of the border may undergo a smooth bifurcation. Taking into account that at a flip bifurcation, $f_R'(x^*_{Rf}) = -\beta\gamma/(x^*_{Rf})^{\gamma+1} = -1$, we obtain the condition $(x^*_{Rf})^{\gamma+1} = \beta\gamma$, or

$$x^*_{Rf} = (\beta\gamma)^{\frac{1}{(\gamma+1)}}. \tag{6}$$

On the other hand, from (5), we get that $f_R'(x^*_R) \geq -1$ for $x^*_R \leq \gamma/\gamma - 1$. Along with (6) the inequality $\beta\gamma \leq (\gamma/\gamma-1)^{\gamma+1}$ holds. Regarding β_R^f as the bifurcation value given in (4), we can state that $f_R'(x^*_R) \geq -1$ iff $\beta \leq \beta_R^f$. Thus, for $\beta > 0$ and $\gamma > 1$, the equation of the smooth flip bifurcation curve, denoted by Ψ_R, can be written in explicit form as follows (see Fig. 2)

$$\Psi_R : \beta = \frac{\gamma^\gamma}{(\gamma-1)^{\gamma+1}}. \tag{7}$$

By substituting (4) into (6), the equation for the fixed point at the flip bifurcation value is obtained as:

$$x^*_{Rf} = \frac{\gamma}{\gamma - 1} > 1. \tag{8}$$

□

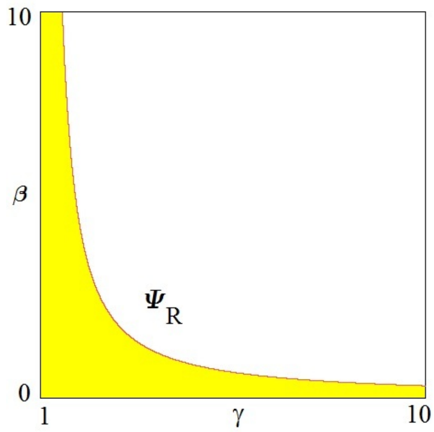

Figure 2: The flip bifurcation curve Ψ_R. Yellow region represents the stability region of the fixed point on the R side.

It is worth to note that the flip bifurcation of the fixed point x^*_R in map f occurs independently on the value of the parameter α ($\alpha \gtreqless 0$). In particular, we demonstrate that system (2) undergoes a flip bifurcation at (x^*_{Rf}, β_R^f). Generically, a flip bifurcation is characterized by the loss of stability of a periodic orbit as a parameter crosses a critical value from above or below. The flip bifurcation is supercritical if, locally, there exist stable periodic orbits with double the period for parameter values near the critical value forming a new branch that emerges at this value. If unstable periodic orbits with double the period coalesce with and are destroyed by stable periodic orbits, the flip bifurcation is subcritical. Now, one can mention that the flip bifurcation of map f in (2) is supercritical since for any fixed value $\gamma > 1$, the fixed point x_R^* is attracting for $0 < \beta \leq \beta_R^f$ and repelling for $\beta > \beta_R^f$.

Theorem 2 *Let $\alpha \in \mathbb{R}$, $\beta > 0$ and $\gamma > 1$. Then the map f given in (2) undergoes a supercritical flip bifurcation at the fixed point (x_{Rf}^*, β_R^f).*

Proof. In order to find out which kind of the flip bifurcation (subcritical, supercritical or degenerate) of the fixed point occurs, we should consider the second iterate of the function $f_R(x)$ in (2), namely,

$$f_R^2(x) = f_R \circ f_R(x) = \frac{\beta}{\left(\frac{\beta}{x^\gamma} + 1\right)^\gamma} + 1,$$

and determine the sign of the third derivative of the function $f_R^2(x)$, calculated at the fixed point $x = x_{Rf}^*$ in (8) and at the bifurcation value $\beta = \beta_R^f$. Recall that (see, for example, [24]):

- if $(f_R^2)'''(x_R^*) < 0$, then the flip bifurcation of the fixed point is *supercritical*;
- if $(f_R^2)'''(x_R^*) > 0$, then the flip bifurcation of the fixed point is *subcritical.*

For the sake of simplicity, we can use the notation F instead of f_R and F^2 instead of f_R^2. Hence, we get

$$(F^2)'''(x) = F'''(F(x))(F'(x))^3 + 3F'(x)F''(x)F''(F(x)) + F'(F(x))F'''(x)$$

which should be evaluated at (8). Since

$$\begin{aligned}
F(x_R^*) &= x_R^*,\\
F'(x_R^*) &= -1,\\
F''(x_R^*) &= -F'(x_R^*)\frac{\gamma+1}{x_R^*} = \frac{\gamma+1}{x_R^*},\\
F'''(x_R^*) &= -F''(x_R^*)\frac{\gamma+2}{x_R^*} = -\frac{\gamma+1}{x_R^*}\frac{\gamma+2}{x_R^*},
\end{aligned}$$

we have

$$\begin{aligned}
(f_R^2)'''(x_R^*) &= \frac{\gamma+1}{x_R^*}\frac{\gamma+2}{x_R^*} - 3\frac{\gamma+1}{x_R^*}\frac{\gamma+1}{x_R^*} + \frac{\gamma+1}{x_R^*}\frac{\gamma+2}{x_R^*}\\
&= 2\frac{\gamma+1}{x_R^*}\frac{\gamma+2}{x_R^*} - 3\frac{\gamma+1}{x_R^*}\frac{\gamma+1}{x_R^*}\\
&= \frac{\gamma+1}{(x_R^*)^2}(2(\gamma+2) - 3(\gamma+1))\\
&= \frac{\gamma+1}{(x_R^*)^2}(1-\gamma).
\end{aligned}$$

Therefore, we can state that for $\gamma > 1$, it holds $(f_R^2)'''(x_R^*) < 0$, and this completes the proof. Note that crossing the flip bifurcation curve Ψ_R from the stability region, the fixed point becomes repelling leading to an attracting 2-cycle. $\square$

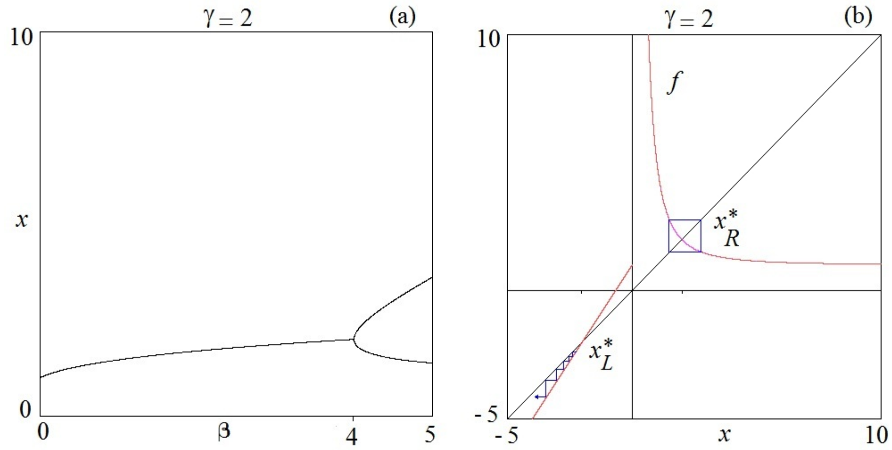

Figure 3: (a) Example of 1D bifurcation diagram β vs x in map f, showing the supercritical bifurcation of x_R^*, for $0 < \beta < 5$, $\alpha = 1.5$, $\gamma = 2$; (b) map f at the bifurcation value $\gamma = 2$, $\beta = 4$, $\alpha = 1.5$.

As an example of 1D bifurcation diagram β vs x in map f, it is shown in Fig. 3 the supercritical bifurcation of x_R^* for the parameter values $\gamma = 2$, $\alpha = 1.5$, $\beta \in [0, 5]$. Also, divergence trajectory on the L side and an attracting 2-cycle on the R side are shown.

3 Divergent dynamics

Now recall that the PWS map in (2) has a discontinuity point at $x = 0$; that is also a vertical asymptote for the function on the right side. For this map, the fixed point on the left side of the border is expressed as

$$x_L^* = -\frac{1}{\alpha - 1} < 0,$$

which exists obviously for $\alpha > 1$, and it is a repelling fixed point. Therefore, divergent trajectories certainly exist, with immediate basin $(-\infty, x_L^*)$.

Differently, in the parameter range $\alpha < 1$, in which the slope of the straight line is not larger than 1, no fixed point exists on the L side. Hence, for $\alpha < 0$, any point on the left side is mapped in the R side in one iteration. Also, for $0 < \alpha \leq 1$, we can see that any point on the left side has an increasing sequence reaching to the right side. That is, the trajectories cannot be divergent.

As mentioned above, for $\alpha > 1$, due to the existence of the repelling fixed point x_L^*, the vertical asymptote is mainly related to divergent trajectories. In fact, a set of positive measure of points with divergent dynamic behavior exists, denoted B_∞ (basin of $-\infty$ or set of divergent trajectories). We can state that $-\infty$ is attracting with total basin $(-\infty, x_L^*)$, so that

$$B_\infty = (-\infty, x_L^*) = \left(-\infty, -\frac{1}{\alpha - 1}\right),$$

while any point belonging to the interval $(x_L^*, 0)$ has a trajectory which goes to the right side in a finite number of iteration. An example is shown in Fig. 3b.

One more feature that is worth to mention is that, any initial condition on the L side for $x > x_L^*$ has a trajectory ending to the R side from which cannot escape. In fact, any initial condition $x > 0$ has a trajectory which cannot leave the right side and converges either to the attracting fixed point or to an attracting 2-cycle. Moreover, note that for $\gamma < 1$, any point on the right side converges to the attracting fixed point x_R^*, and the basin of attraction of x_R^* for $\alpha \leq 1$ is $(-\infty, +\infty)$, while for $\alpha > 1$, it is $(x_L^*, +\infty)$. Besides, for $\gamma > 1$ and $0 < \beta < \gamma^\gamma/(\gamma - 1)^{\gamma+1}$ (therefore, the fixed point x_R^* is attracting), we have the same dynamics as for $\gamma < 1$, while increasing β, we have an unstable fixed point and an attracting 2-cycle whose basin of attraction is $(-\infty, +\infty)\backslash\{x_R^*\}$ for $\alpha \leq 1$ while for $\alpha > 1$, it is $(x_L^*, +\infty)\backslash\{x_R^*\}$.

4 Conclusion

In this study, we investigated the dynamics of a 1D discontinuous PWS map f in (2), recently introduced as a dynamic model in engineering sciences, with real exponent $\gamma > 0$, which leads to the existence of a vertical asymptote for map f. In this paper, the parameter space includes $\mu > 0$ and $\beta > 0$, that has not been examined in the previous publications. Using α and β as our bifurcation parameters, we proved that depending on the parameter γ, different bifurcation structures occured. For $0 < \gamma < 1$, our numerical results, as well as rigorous proofs, indicated that the dynamical behaviour of map f is simple while for $\gamma > 1$, the bifurcation structure is related to the supercritical flip bifurcation of the fixed point on the right side of the border. For $\beta > 0$, we proved that the map can have only period-1 orbit of double periods. The equation of the flip bifurcation curve has been given as well. Finally, we noted that due to the existence of a repelling fixed point x_L^*, for $\alpha > 1$, divergent trajectories exist. Hence, it is stated that a set of positive measure of points with divergent trajectories must exist.

References

[1] S. Banerjee and C. Grebogi, Border collision bifurcations in two-dimensional piecewise smooth maps, Phys. Rev. E, **59** (1991), pp. 4052–4061. https://doi.org/10.1103/physreve.59.4052

[2] S. Banerjee, M. S. Karthik, G. H. Yuan, and J. A. Yorke, Bifurcations in one-dimensional piecewise smooth maps: Theory and applications in switching circuits, IEEE Trans. Circuits Sys. I: Fundam. Theory Appl., **47** (2000), no. 3, pp. 389–394. https://doi.org/10.1109/81.841921

[3] S. Banerjee and G. C. Verghese, *Nonlinear phenomena in power electronics: Attractors, bifurcations, chaos, and nonlinear control*, New York: Wiley-IEEE Press, 2001.

[4] C. M. Berger, X. Zhao, D. G. Schaeffer, H. M. Dobrovolny, and D. J. Krassowska Wand Gauthier, Period-doubling bifurcation to alternans in paced cardiac tissue: Crossover from smooth to border-collision characteristics, Phys. Rev. Lett., **99** (2007), 058101. https://doi.org/10.1103/physrevlett.99.058101

[5] H. Dankowicz and A. B. Nordmark, On the origin and bifurcations of stick–slip oscillations, Physica D, **136** (2000), no. 3–4, pp. 280–302. https://doi.org/10.1016/s0167-2789(99)00161-x

[6] M. di Bernardo, C. J. Budd, A. R. Champneys, and P. Kowalczyk, *Piecewise-smooth dynamical systems: Theory and applications*, Applied Mathematical Sciences, **163**, Springer-Verlag, London, 2008. https://doi.org/10.1007/978-1-84628-708-4

[7] M. di Bernardo, P. Kowalczyk and A. B. Nordmark, Bifurcations of dynamical systems with sliding: derivation of normal-form mappings, Physica D, **170** (2002), no. 3–4, pp. 170–175. https://doi.org/10.1016/s0167-2789(02)00547-x

[8] L. Gardini, V. Avrutin, I. Sushko, and F. Tramontana, Continuous and discontinuous piecewise-smooth one-dimensional maps: Invariant sets and bifurcation structures, World scientific series on nonlinear science, Series A: vol. 95, 2019. https://doi.org/10.1142/8285

[9] L. Gardini and R. Makrooni, Necessary and sufficient conditions of full chaos for expanding Baker-like maps and their use in non-expanding Lorenz maps, Commun. Nonlinear Sci. Numer. Simul., **67** (2019), pp. 272–289. https://doi.org/10.1016/j.cnsns.2018.06.018

[10] L. Gardini, R. Makrooni and I. Sushko, Cascades of alternating smooth bifurcations and border collision bifurcations in a family of discontinuous linear-power maps, Discrete Contin. Dyn. Sys.: Series B, **23** (2018), no. 2, pp. 701–729. https://doi.org/10.3934/dcdsb.2018039

[11] C. Halse, M. Homer and M. di Bernardo, C-bifurcations and period-adding in one-dimensional piecewise smooth maps, Chaos Solit. Fractals, **18** (2003), no. 5, pp. 953–976. https://doi.org/10.1016/s0960-0779(03)00066-3

[12] M. A. Hassouneh and E. H. Abed, Border collision bifurcation control of cardiac alternans, Int. J. Bifurcat. Chaos, **14** (2004), no. 9, pp. 3303–3315. https://doi.org/10.1142/s0218127404011351

[13] A. Kumar, S. Banerjee and D. P. Lathrop, Dynamics of a piecewise smooth map with singularity, Phys. Lett. A, **337** (2005), no. 1–2, pp. 87–92. https://doi.org/10.1016/j.physleta.2005.01.046

[14] R. Makrooni, N. Abbasi, M. Pourbarat, and L. Gardini, Robust unbounded chaotic attractors in 1D discontinuous maps, Chaos Solit. Fractals, **77** (2015), pp. 310–318. https://doi.org/10.1016/j.chaos.2015.06.012

[15] R. Makrooni, L. Gardini, I. Sushko, Bifurcation structures in a family of 1D discontinuos linear-hyperbolic invertible maps, Int. J. Bifurcat. Chaos, **25** (2015), no. 13, 1530039, 21 pp. https://doi.org/10.1142/s0218127415300396

[16] R. Makrooni, F. Khellat and L. Gardini, Border collision and fold bifurcations in a family of one-dimensional discontinuous piecewise smooth maps: Divergence and bounded dynamics, J. Differ. Equ. Appl., **21** (2015), no. 9, pp. 791–824. https://doi.org/10.1080/10236198.2015.1046855

[17] R. Makrooni, F. Khellat and L. Gardini, Border collision and fold bifurcations in a family of one-dimensional discontinuous piecesiwe smooth maps: Unbounded chaotic sets, J. Differ. Equ. Appl., **21** (2015), no. 8, pp. 660–695. https://doi.org/10.1080/10236198.2015.1045893

[18] A. B. Nordmark, Non-periodic motion caused by grazing incidence in an impact oscillator, J. Sound Vib., **145** (1991), no. 2, pp. 279–297. https://doi.org/10.1016/0022-460x(91)90592-8

[19] E. Pavlovskaia, M. Wiercigroch and C. Grebogi, Two-dimensional map for impact oscillator with drift, Phys. Rev. E, **70** (2004), 036201. https://doi.org/10.1103/physreve.70.036201

[20] E. Pavlovskaia and M. Wiercigroch, Low-dimensional maps for piecewise smooth oscillators, J. Sound Vib, **305** (2007), no. 4–5, pp. 750–771. https://doi.org/10.1016/j.jsv.2007.04.044

[21] M. Pourbarat, N. Abbasi and R. Makrooni, Chaos in smooth piecewise dynamical systems with one discontinuous point, J. Adv. Math. Model., **9** (2019), no. 2, pp. 93–105.

[22] R. Sharan and S. Banerjee, Character of the map for switched dynamical systems for observations on the switching manifold, Phys. Lett. A, **372** (2008), no. 23, pp. 4234–4240. https://doi.org/10.1016/j.physleta.2008.03.050

[23] W. T. Shi, C. L. Gooderidge and D. P. Lathrop, Viscous effects in droplet-ejecting capillary waves, Phys. Rev. E, **56** (1997), 4157. https://doi.org/10.1103/physreve.56.472

[24] S. Wiggins, *Introduction to applied nonlinear dynamical systems and chaos*, Springer-Verlag, New York, 2003.

Roya Makrooni
Faculty of mathematics, statistics and computer sciences,
University of Sistan and Baluchestan,
University Blvd, Zahedan, Iran.
r.makrooni@math.usb.ac.ir

Please, cite to this paper as published in
Armen. J. Math., V. **14**, N. 13(2022), pp. 1–12
https://doi.org/10.52737/18291163-2022.14.13-1-12